Assessing maximum amplitude and corresponding frequency for vortex-induced vibrations

Øyvind Mortveit Ellingsen, Xavier Amandolese, Pascal Hémon

Assessing maximum amplitude and corresponding frequency for vortex-induced vibrations

Øyvind Mortveit Ellingsen [1,2], Xavier Amandolese [2,3], Pascal Hémon [2]

[1] *CAPE , CSTB, Nantes , France, oyvind@ladhyx.polytechnique.fr*
[2] *LadHyX, CNRS-École Polytechnique, Palaiseau, France*
[3] *LMSSC, CNAM, Paris , France*

Abstract
Vortex-induced vibrations can damage structures exposed to cross-flows. The current design estimates of structural amplitude are based on structural nonlinearity but we will here derive a different estimate based on a coupled system with nonlinear fluid forcing. Two estimates of maximum structural amplitude is investigated based on approximations the coupled system and fluid speed at maximum amplitude. Our result shows that both estimates are close to the maximum amplitude found using numerical integration but that the predicted fluid speed differs. With further refinement, the result presented may prove useful in designing structures to withstand vortex-induced vibrations.

Keyword: Vortex-induced vibrations, nonlinear approximation, design estimates, prediction error

1 Introduction

Structures in cross-flow will experience unsteady periodic, loading due to shedding of vortexes (Blevins, 2001) that can lead to severe vortex-induced vibrations (VIV). For a designer, there are two useful pieces of information: when vibrations occurs and how severe vibration amplitudes are. These information pieces enables us to find the lifetime of a structure and to design a good tuned-mass damper.

When designing structures to withstand these aerodynamic loads, simple estimates of loading and response reduces the time spent iterating designs. In the Eurocode (2010) and CICIND (2010) building codes, structural excitation due to VIV is modeled using random vibration theory and a simplified structural nonlinearity (Vickery and Basu, 1983). This simplified model is made for the design offices of the early 1980s and often only the maximum response is found.

Another approach in modeling VIV is to couple a structural equation with a nonlinear equation describing or mimicking the vortex forcing. This approach was used Facchinetti et al. (2004) and several other researchers before them (Païdoussis et. al, 2010). A benefit of Facchinetti's model is that it has a simple but powerful coupling between wake and structure. The problem is that it's a set of nonlinear differential equations. This is numerically solvable but work is needed to make it as simple and useful as the current design model.

Why should a designer consider using something other than the existing design model? According to Lupi et al. (2018), it is overly conservative and can be unrealistic for many

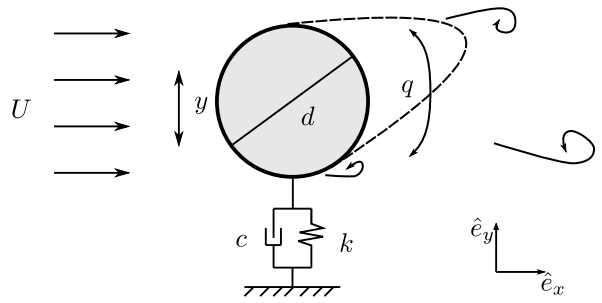

Figure 1 – Sketch of the vortex-induced vibration system

designs. This is partly due to the formulation of the method and the parameters used; their effect is especially prevalent at low Scruton numbers.

We will take steps to address the above concerns by creating a new predictive model that perform better at low Scruton number (Sc<10). Based on an approximation of structural and forcing amplitudes, we will define two approximations of the fluid speed at maximum response. The speed estimates is then plugged back into the amplitude approximates. Amplitude and speed results from both estimates will then be compared with numerical simulations.

2 Vortex-induced vibrations model and approximation

2.1 Model definition

Fig 1 shows a simple system experiencing vortex-induced vibrations. The structure is left free to vibrate in the $\hat{e}_y$ direction and the wake oscillates on it. This has been modeled using a combination of a linear structural oscillator and a nonlinear wake oscillator shown respectively in Eqs. 1 and 2 below

$$\ddot{y}+D\dot{y}+y=\omega_q^2 Mq, \tag{1}$$

$$\ddot{q}+\epsilon\left(q^2-1\right)\dot{q}+\omega_q^2 q=A\ddot{y}. \tag{2}$$

where the variables y and q are dimensionless. Here, A and ϵ are experimentally determined constants and M is the unsteady lift force, F, scaled by the mass-ratio μ ($M=F/\mu$). The parameters D, F and μ as defined as

$$\mu=\frac{m+0.25\pi\rho d^2 C_m}{\rho d^2}, \tag{3}$$

$$D=2\zeta+\frac{C_D}{4\pi\mu St}, \tag{4}$$

$$F=\frac{C_{Lo}}{16\pi^2 St^2}, \tag{5}$$

m is structural mass per unit length, ρ fluid density, d diameter, ζ critical damping ratio and St Strouhal number. C_m, C_D and C_{Lo} are the added mass, mean drag and unsteady lift amplitude coefficients respectively.

One variable is undefined and it's one of the most important: the fluid speed variable ω_q. It's defined as the product of the reduced velocity based on the structure's natural frequency and the Strouhal number ($\omega_q = U_R St$). It is therefore a reduced fluid frequency equivalent to the ratio of shedding frequency to the natural structural frequency.

If we assume that the equations are weakly nonlinear, then they can be approximated. This system can be shown to have the approximate steady-state solutions below when using the method of averaging:

$$r_y(\omega_q, \theta) = 2\frac{\omega_q^2 M}{D}\left[1 + \frac{\omega_q AM \sin(\theta)}{\epsilon D}\left(\sin(\theta) - D\cos(\theta)\right)\right]^{0.5} \sin(\theta), \tag{6}$$

$$0 = \omega_q^2(1 - AM) - 1 + \omega_q^2 AM \sin^2(\theta) + \left(\frac{D}{\sin(\theta)} + \frac{\omega_q^2 AM}{D}\sin(\theta)\right)\cos(\theta). \tag{7}$$

where r_y is the structural amplitude and θ is the phase difference between q and y, i.e. phase difference between force and motion. Notice that there is no equation for the wake amplitude. As the structural equation and coupling is linear, the equations for wake amplitude can be expressed as a function of phase difference only. This then enables us to write the structural amplitude as a function of phase difference only.

2.2 Amplitude scaling

If we ignore the square root term and the last $\sin\theta$ term in Eq. Eq. 6, we get an equation that depend linearly on the ratio of M to D. If we expand this ratio, we get the scaling relationship

$$r_y \propto \frac{2\pi F}{Sc + 2\pi^2\zeta + \frac{C_D}{2St}}. \tag{8}$$

where Sc is the Scruton number defined as

$$Sc = \frac{4\pi\zeta m}{\rho d^2}. \tag{9}$$

In words, predicted amplitude is dependent on four parameters: geometry, mass, structural damping and aerodynamics. This differs from some previous notions on maximum amplitude scaling. However, it corroborates the opinion that combining mass and damping into a parameter is arbitrary (Sarpkaya 2004).

2.3 Model validation

To find the amplitude at a given speed, the first step is to find the phase difference using Eq. 7. This may look daunting, but it can be rewritten to a cubic equation. One of the closed form solutions corresponds to the high amplitude VIV response, another to low amplitude and the last to an unstable solution. Only the phase differences between 0 and 180° are used.

A "postcritical Reynolds" experiment with dampers by Belloli et al. (2015) is used for validation and for comparison with the maximum amplitude of the CICIND model (2010). See Tab. 1 for parameters. Fig. 2 shows the comparison and the design code over predict by more than a factor of 2. Our model does well at $\omega_q < 1$ and less well above. The maximum amplitude between experiment and model is similar as is the range of high amplitude vibrations.

Table 1 – Parameters used to compare the approximations and the numerical results.

Case	ϵ	A	γ	F	ζ	d	ρ
Exp.	0.3 [-]	12 [-]	0.479 [-]	0.0401 [-]	0.01200 [-]	0.72 [m]	1.225 [kg/m^3]
Low dam	0.3 [-]	12 [-]	0.442 [-]	0.0401 [-]	0.00191 [-]	2.00 [m]	1.225 [kg/m^3]
High damp	0.3 [-]	12 [-]	0.442 [-]	0.0401 [-]	0.00955 [-]	2.00 [m]	1.225 [kg/m^3]

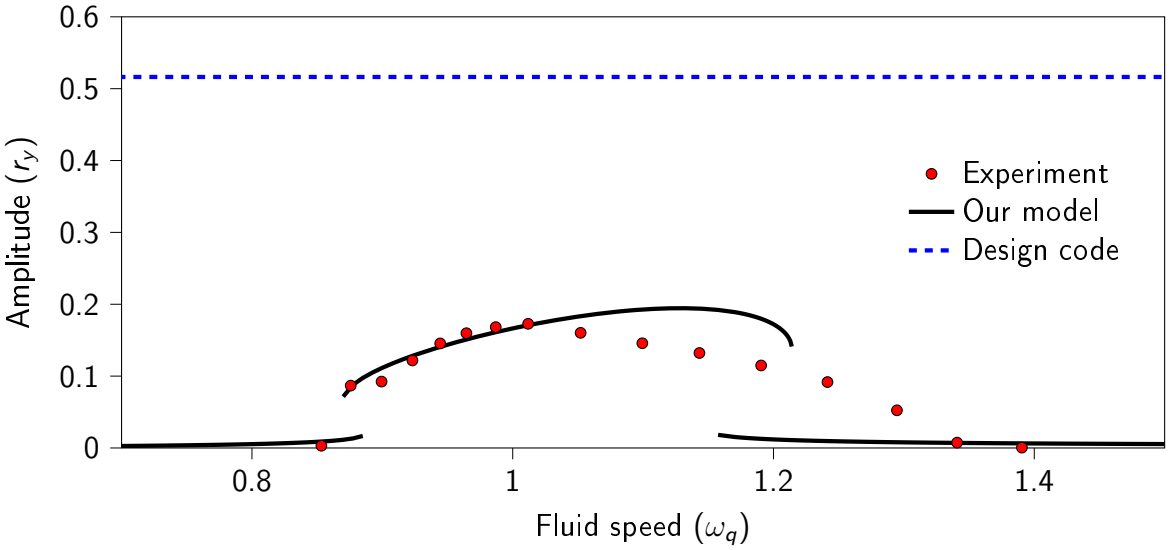

Figure 2 – Comparison of models and experiment of Belloli et al. (2015)

3 Estimates of maximum

3.1 The approximations

Two different approximates of the frequency at maximum amplitude are tested:

$$\omega_{q1} = \frac{1}{1-\sqrt{AM}}, \tag{10}$$

$$\omega_{q2} = \sqrt{\frac{D\left(\sin\left(\theta\right) - D\cos\left(\theta\right)\right)}{AMD\sin\left(\theta\right)^3 + AM\cos\left(\theta\right)\sin\left(\theta\right)^2 + D\left(1-AM\right)\sin\left(\theta\right)}}. \tag{11}$$

The first approximate (Eq. 10), dubbed "method 1", is based on the work of de Langre (2006). Our guess is that maximum amplitude corresponds to the upper limit of the linear synchronization definition. In terms of Fig. 2, this corresponds to the start of our rightmost low amplitude solutions. Method 1 is independent of the structural damping parameter D and depends only on the coupling terms associated with forcing.

The second approximate, "method 2", is based on assuming that maximum response coincide with a specific phase difference. The form of method 2 is shown in Eq. 11 and includes structural damping and the forcing terms. An added benefit of this approach, is that it reduces the calculation process to one longer equation; we are assuming we know θ, so there is no need to calculate the value. By inspection, the phase difference at maximum response is $\approx 0.65\pi$.

The estimates of maximum amplitude and dimensionless fluid speed are compared to results from numerical simulations at several Sc using two damping cases. One corresponds to a low damping case and the other to a high damping. The values of μ are inferred from Sc using the constants given in Tab. 1 and Eqs. 3 and 9. For comparison, both absolute values and the relative difference in percentage are used in the next two subsections.

3.2 Approximation of fluid speed at maximum response

The evolution of dimensionless fluid speed as a function of Sc when structural damping is low is shown in Fig. 3. When comparing the results using method 1 and numerical, it is easy to spot differences. Predicted speed changes differently with Scruton number and the values are inconsistent for method 1 and numerical. The approximate speed using method 2 is consistently higher than the numerical result but does drop similarly with increasing Sc.

To further evaluate the approximations, a second damping case is studied. The evolution of fluid speed at maximum response when damping is five times greater is shown in Fig. 4. With the higher damping, predicted speed drops similarly for method 1 and numerical although the predicted speed is consistently much higher. Increasing damping barely changed the differences between numerical results and method 2. The main difference would be a slightly increased difference in predicted value.

3.3 Maximum response

Maximum response is predicted to decrease similarly to how the fluid speed at maximum response drops, i.e. like Sc^{-1}. This gives a rapid drop in predicted vibration amplitude as seen in Figs. 5 and 6 showing the progression for the lightly and higher damped cases respectively.

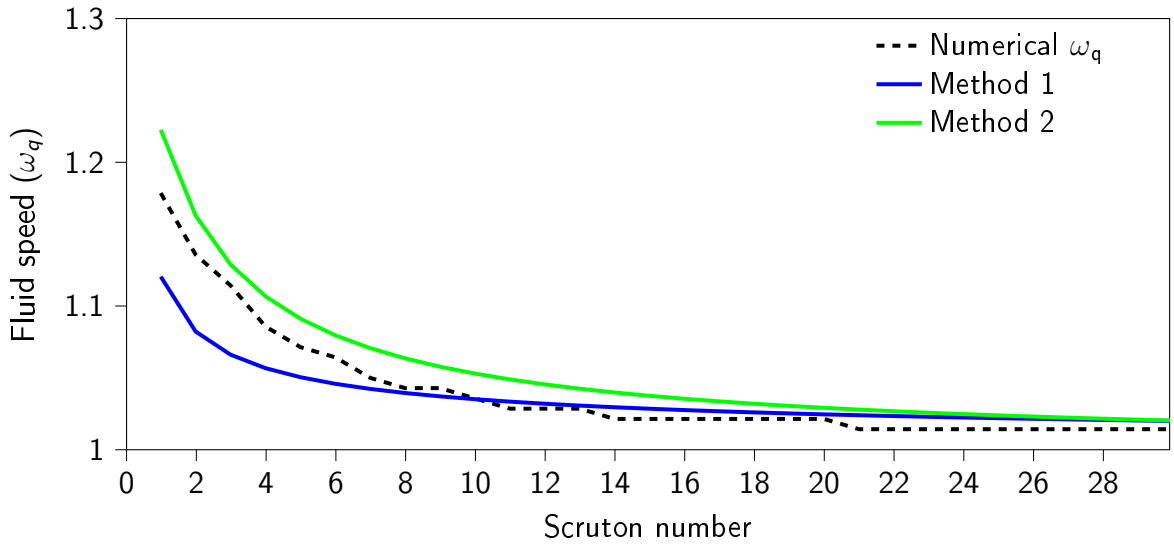

Figure 3 – ω_q corresponding to maximum r_y for low damping case

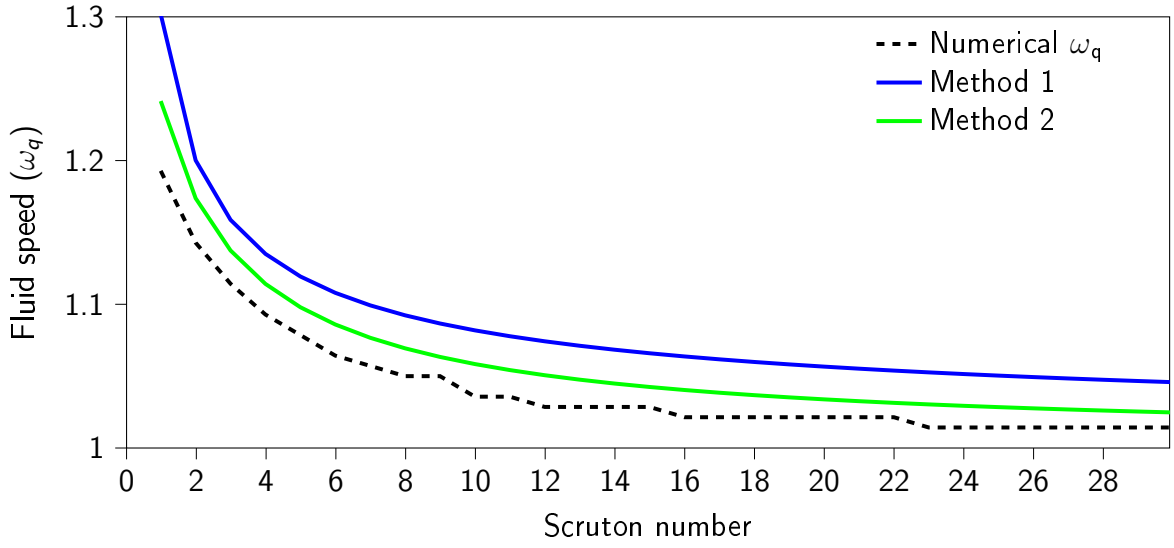

Figure 4 – ω_q corresponding to maximum r_y for high damping case

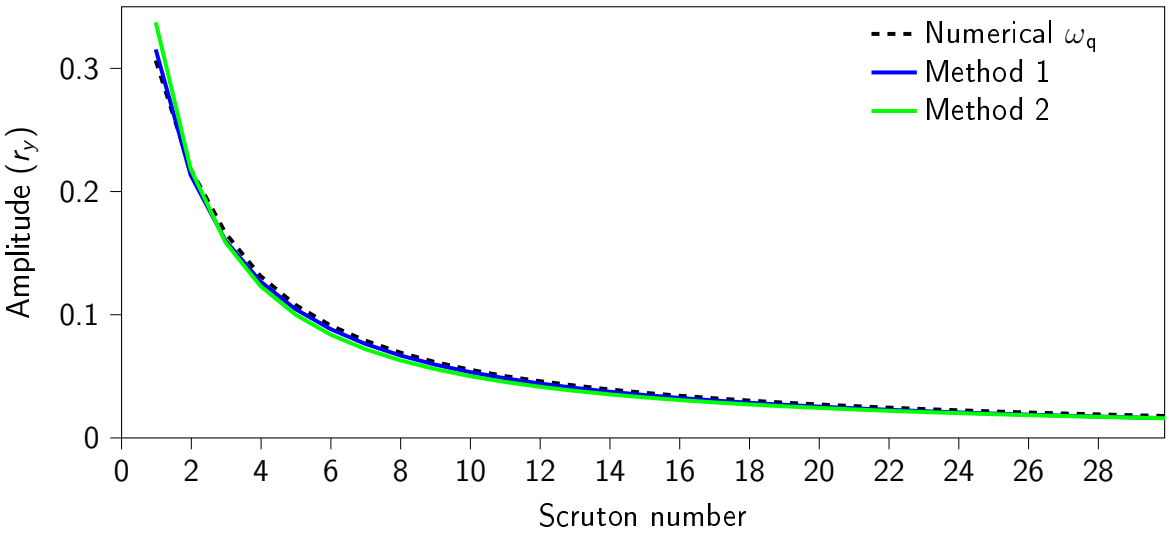

Figure 5 – Comparison of maximum response amplitude using approximates and numerical integration at low structural damping

Even with the difference in predicted speed, method 1 predict similar amplitudes as the numerical results for most tested Scruton numbers in the lightly damped case. This could be an indication of low sensitivity in fluid speed when it comes to estimating maximum amplitude. For the higher damped case, this is not true. At Scruton numbers below 2, the amplitude becomes noticeably over predicted and then under predicts for all Scruton numbers. The more egregious error, is that the predicted speed corresponds to the low amplitude solution for Scruton numbers higher than nine.

Method 2 performs similarly to method 1 for the lightly damped case but with a difference, the predicted amplitude is noticeably higher at $Sc = 1$. The real point of improvement is in the higher damped case. While it has the same over predicting behavior at Scruton numbers below 2, the predicted amplitude is close to the numerical results for all other tested Scruton numbers. In other words, the maximum speed predicted is within the VIV region and close to the amplitude peak.

At the shown damping levels, method 1 performed passably for Scruton numbers less than 10. If we increase the damping, method 1 eventually under predicts for all Scruton numbers. The best estimate of maximum amplitude and fluid speed at maximum is method 2 which is based on assuming we know the phase difference that give maximum amplitude. The results are promising and in the next section we will further explore the usefulness of our estimate.

4 Applicability of our estimate of maximum amplitude

We have so far compared the absolute differences between our approximates and the numerical results for two different damping levels. This section is focused on the applicability of our predictions and a comparison with other predictive models, more specifically the model of Vickery and Basu used in building codes (CICIND, 2010; Eurocode, 2010).

As seen in section 2.3 and Fig. 2, there is room for improvement in the models used in the

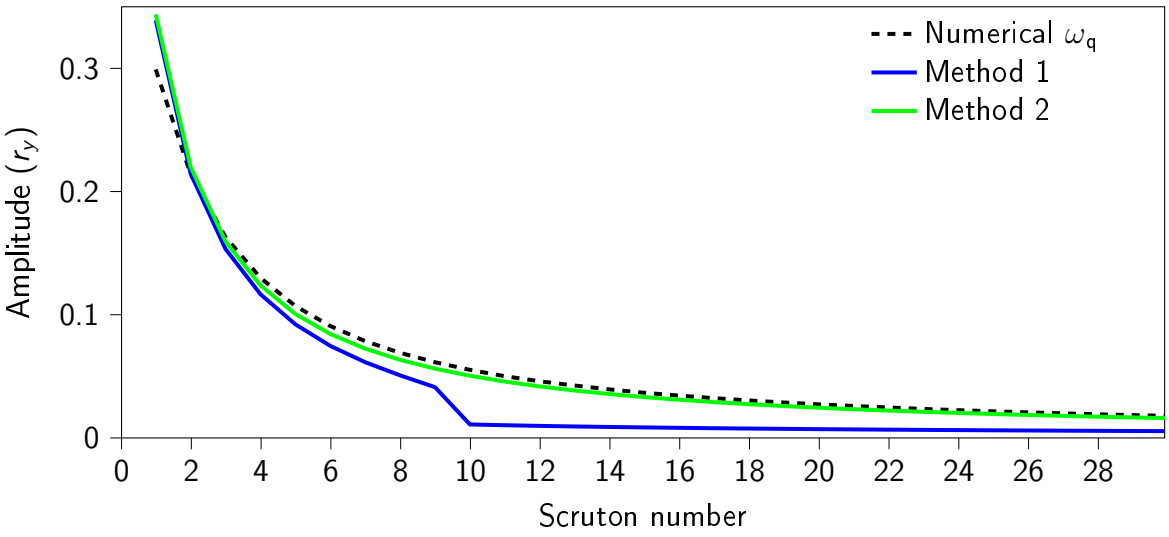

Figure 6 – Comparison of maximum response amplitude using approximates and numerical integration at high structural damping

mentioned building code. We will focus on two connected, negative properties. The first of them, is that they tend to be overly conservative in estimating amplitudes. Lupi et al. (2017) studied the difference between predicted and actual VIV amplitude and found that the predicted amplitude tended to be much larger than the actual vibration amplitude.

The second property has to do with predictive amplitude as a function of Scruton number (Lupi et al., 2017). The formulation used in the building codes can have abrupt jumps in predicted amplitude when slightly changing structural damping or aerodynamics. This is associated with a critical Scruton number that marks the transition from positive linear structural damping to negative. High amplitude prediction can also be connected with the imposed negative aerodynamic damping effect.

Our estimates of maximum amplitude follows a different trend and there is a smooth increase in predicted amplitude as Scruton number decreases without abrupt jumps. Our predicted maximum amplitude can have large changes with Scruton number at $Sc < 2$, but this is not as pronounced as the behavior of the design models..

How applicable is our two dimensional model in predicting the dynamic response of a three dimensional structure? Due to three dimensional effects, lengthwise force correlation and structural mode shapes, it is not unthinkable that our predictions will be wrong. But it may be possible to simplify and include the mentioned effects into our model. If we follow the same reasoning as Vickery and Basu (1983), we can modify our lift force by assuming a constant average speed over the top part of the cylinder. The lift force is then weighted and integrated over the cylinder length with a weighting factor proportional to the structural mode shape.

Another aerodynamic effect not accounted for in our model, but is in the design models, is the effect of turbulence and noise on the prediction. We can theoretically get the response amplitude using unsteady aerodynamic coefficients measured in turbulent conditions, but predicting the correct wind speed is harder; amplitude might be correct but the speed not. Getting the correct coefficients at super-critical (or "postcritical") Reynolds numbers is another story

and requires extensive work.

5 Conclusions

Two estimates of maximum structural amplitude due to vortex-induced vibrations has been tested and shown to accurately estimate maximum response. The best of the two is to assume that maximum amplitude occurs at a predefined phase difference between forcing and motion. Using a phase difference of $\theta = 0.65\pi$ gives an approximate fluid speed at maximum response slight higher than numerical results but similar evolution with Scruton number. The difference in fluid speed has a small effect on the difference in predicted maximum amplitude and the numerical result and estimate are similar.

References

Belloli, M., Giappino, S., Morganti, S., Muggiasca, S., Zasso, A., 2015. Vortex induced vibrations at high Reynolds numbers on circular cylinders. Ocean Eng, 94, 140–154.

Blevins, R. D., 2001. Flow-Induced Vibration (2nd ed.). Krieger Pub Co., Malabar, FL.

CICIND, 2010. CICIND Model Code for Steel Chimneys: September 2010 Revision 2. CICIND.

de Langre, E., 2006. Frequency lock-in is caused by coupled-mode flutter. J Fluids Struct, 22(6–7), 783–791.

Eurocode., 2010. 1: Actions on structures, Part 1–4: General Actions (EN–1991). Eurocode.

Facchinetti, M.L., de Langre, E., Biolley, F., 2004. Coupling of structure and wake oscillators in vortex-induced vibrations. J Fluids Struct, 19(2), 123–140.

Païdoussis, M. P., Price, S. J., de Langre, E., 2010. Fluid-Structure Interactions Cross-Flow-Induced Instabilities. Cambridge University Press., Cambridge, NY.

Sarpkaya, T., 2004. A critical review of the intrinsic nature of vortex-induced vibrations. J Fluids Struct, 19(4), 389–447.

Vickery, B.J., Basu, R., 1983. Simplified approaches to the evaluation of the across-wind response of chimneys.J Wind Eng Ind Aerod, 14(1), 153–166.